

T. Schmid · C. Helmbrecht · C. Haisch · U. Panne
R. Niessner

On-line monitoring of opaque liquids by photoacoustic spectroscopy

Received: 5 September 2002 / Revised: 4 November 2002 / Accepted: 16 December 2002 / Published online: 22 February 2003
© Springer-Verlag 2003

Abstract A new photoacoustic sensor system for on-line monitoring of highly concentrated and optical opaque liquid samples is presented. The dyeing of textiles is performed with highly concentrated dye solutions with concentrations ranging from 50 mg L⁻¹ up to 40 g L⁻¹. For process optimization and control of the wastewater, an on-line monitoring of the dye concentration is needed. Optical transmission measurements allow the determination of the dye concentration in a relatively small range. Samples with concentrations in the upper mg L⁻¹ and g L⁻¹ range have to be diluted before the measurement due to their optical opacity. Additionally, light-scattering particles have a strong effect on the transmitted light intensity. By photoacoustic spectroscopy, concentrations in condensed matter can be determined over several orders of magnitude. Furthermore, scattering particles do not generate any photoacoustic signal.

Keywords Photoacoustic spectroscopy · Opaque liquids · Textile dyes · On-line monitoring

Introduction

The dyeing of textiles is performed with highly concentrated dye solutions with concentrations from 50 mg L⁻¹ up to 40 g L⁻¹. To achieve satisfactory results, in most cases mixtures of 2–4 textile dyes are used. In addition to soluble reactive or direct dyes, the dyeing of textiles is performed with suspended dispersion dyes [1].

For process optimization and control of the wastewater, an on-line monitoring of the dye concentration is required. The classical measurement techniques based on optical transmission are hampered by a limited dynamic range. Samples with concentrations in the upper mg L⁻¹

and g L⁻¹ range have to be diluted before the measurement due to their optical opacity. Additionally, light-scattering particles have a strong effect on the transmitted light intensity. Attenuated total reflectance (ATR) probes can provide a relatively wide dynamic range, but they are also affected by scattering particles.

Photoacoustic spectroscopy (PAS) has been extensively used for nondestructive investigations in chemical, biological, and environmental studies [2]. PAS allows the determination of concentrations in condensed matter over several orders of magnitude. Even absorption coefficients of optical opaque samples can be determined by pulsed photoacoustic spectroscopy without any dilution [3]. Furthermore, scattering particles do not generate any photoacoustic signal. In this communication, new photoacoustic sensor systems for on-line monitoring of highly concentrated and optical opaque samples are presented.

Photoacoustic spectroscopy

Pulsed photoacoustic spectroscopy is based on the absorption of short laser pulses inside condensed matter. If radiative relaxation processes (e.g., fluorescence, phosphorescence) can be neglected, the absorbed energy is converted exclusively into heat. Due to the thermal expansion of the medium, pressure waves are generated which can be detected by piezoelectric transducers [2, 4]. In the case of pressure detection in aqueous systems, the transducer is termed hydrophone.

The energy absorbed inside an irradiated medium having the optical absorption coefficient α is

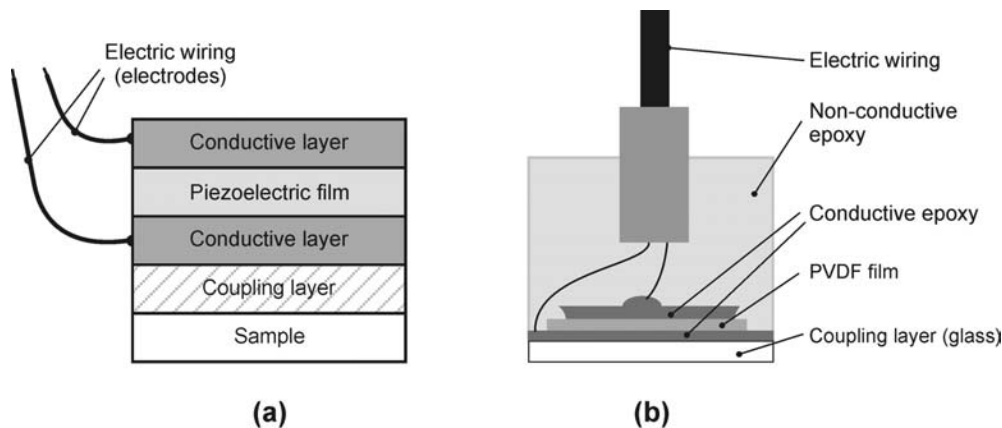
$$Q_{abs}(l) = Q_0 (1 - e^{-\alpha l}) \quad (1)$$

where Q_0 is the laser pulse energy and l is the distance from the sample surface along the laser beam. For $\alpha l \ll 1$, Eq. (1) can be approximated by a linear function and the amplitude p of the photoacoustic signal can be described by

$$p \propto \frac{\beta c^2}{C_p} Q_0 \alpha, \quad (2)$$

T. Schmid · C. Helmbrecht · C. Haisch (✉) · U. Panne
R. Niessner
Institute of Hydrochemistry, Technical University of Munich,
Marchioninstraße 17, 81377, Munich, Germany
e-mail: Christoph.Haisch@ch.tum.de

Fig. 1a,b Schematic setup of a hydrophone based on a piezoelectric polymer film (a) and setup of the hydrophone used in this study (b)



where β is the thermal expansion coefficient, c is the speed of sound, C_p is the heat capacity, Q_0 is the pulse energy, and α is the absorption coefficient of the sample [4]. The optical absorption coefficient depends on the wavelength and is proportional to the concentration of the absorbing analyte.

Depending on the optical absorbance of the medium, different acoustic waveforms are generated. In weakly absorbing samples, the volume irradiated by a collimated beam is approximately cylindrical. Therefore, cylindrical waves are formed which propagate perpendicularly to the laser beam. With increasing optical absorbance, optical penetration depth and irradiated volume decreases. In highly absorbing and optical opaque samples, spherical waves are generated [5]. Thus, if the absorption coefficient varies over several orders of magnitude, different waveforms are generated and a linear relation between photoacoustic signal amplitude and concentration according to Eq. (2) cannot be expected for the whole concentration range.

For the detection of laser-induced pressure pulses, piezoelectric transducers are preferably used due to the restricted bandwidth of microphones. For the analysis of liquid samples, a chemically inert coupling layer between sample and transducer is necessary. Additional coupling layers can be integrated into the hydrophone to achieve high acoustic transmission from the liquid sample to the piezoelectric detector. Electrodes on both sides of the piezoelectric transducer are needed for measurement of the voltage generated by the piezoelectric effect.

The essential parameter of a medium determining the transmission and reflection properties with regard to acoustic waves is the acoustic impedance Z :

$$Z = \rho c, \quad (3)$$

where ρ is the density of the medium. If the pressure p_0 reaches an interface between two layers with the acoustic impedances Z_1 and Z_2 respectively, the pressure p_T is transmitted:

$$p_T = p_0 \frac{2Z_2}{Z_2 + Z_1} = p_0 t \quad (4)$$

with t denoting the acoustic transmission factor [6]. To achieve high transmission factors, suitable coupling mate-

rials have to be used. Figure 1a reveals the schematic setup of a hydrophone based on a piezoelectric polymer film.

Materials and methods

Hydrophone

For detection of laser-induced pressure waves, a 25- μm -thick piezoelectric poly(vinylidene fluoride) (PVDF) film (bi-oriented piezoelectric PVDF, Piezotec SA, Saint-Louis, France) was used. The film was circular with a diameter of 8 mm. The PVDF was coupled to a 1-mm-thick circular glass window with a diameter of 10 mm by a conductive epoxy (Fig. 1b). Glass is sufficiently chemically inert and provides good acoustic coupling with water. The acoustic transmission factor between water and glass is 1.8. The conductive epoxy provides both electric and acoustic contact. The electrode was coupled by conductive silver ink to the conductive epoxy layer. The acoustic transmission factor between glass and conductive epoxy is 0.85 and between conductive epoxy and PVDF 0.53. The acoustic transmission efficiency of the system “water/coupling layers/PVDF” can be calculated as the product of the transmission factors which is 0.82 corresponding to a ratio between transmitted and incident pressure of 82%. The second electrode was coupled with conductive epoxy to the other side of the PVDF film.

The electrodes were connected to a BNC cable. The signal was pre-amplified (HCA-100 M-50k-C current amplifier, Femto-Mess-technik, Berlin, Germany) and recorded by a digital storage oscilloscope (TDS 620, Tektronix, Beaverton, USA) in a time-resolved fashion. For improvement of the signal-to-noise ratio, every photoacoustic measurement was averaged over 50 laser pulses. The data acquisition was performed with in-house developed LabVIEW software (LabVIEW 5.1, National Instruments, Austin, USA).

Photoacoustic flow cell

The hydrophone is integrated into a flow cell consisting of brass. Figure 2 exhibits setup and mode of operation of the flow cell. The inner volume of the cell is 0.5 mL. Opposite to the hydrophone, a circular glass window with a diameter of 10 mm is integrated into the cell. The laser beam is focused through the glass window and laser-induced pressure waves are detected by the hydrophone along the beam direction.

The distance between glass window and hydrophone is 10 mm. Perpendicularly to the laser beam, liquid samples can be pumped through the cell. For aqueous samples, the flow through the cell is laminar for volume flows up to 470 mL min^{-1} corresponding to a Reynolds number of 2,500.

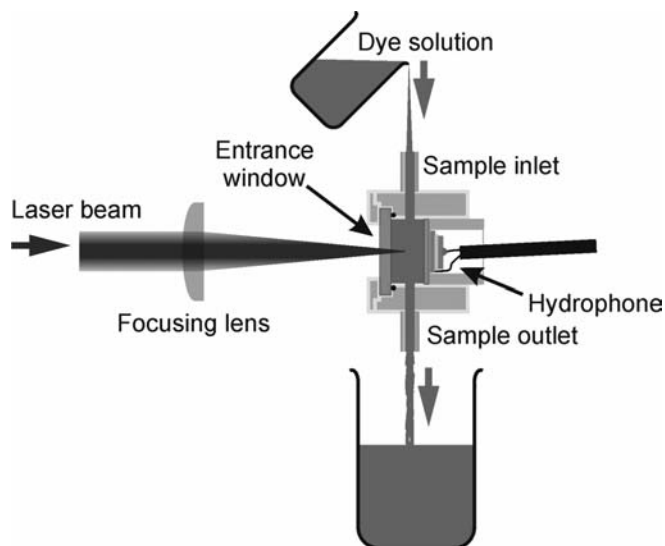


Fig. 2 Setup and principle of operation of the photoacoustic flow cell

Nd:YAG laser system

For calibration of the photoacoustic cell, a Q-switched, frequency doubled Nd:YAG laser (Surelite 10-I, Continuum, Santa Clara, USA) with a repetition rate of 10 Hz mounted on an optical bench was used for excitation at $\lambda = 532$ nm. The laser pulses were attenuated by a beam attenuator (Newport, Irvine, USA), focused by a plano-convex lens ($f = 50$ mm), and coupled into an optical fiber (550- μ m diameter, HCG-MO550T-10, Laser Components, Santa Rosa, USA). At the distal end of the fiber, the beam was collimated by a plano-convex lens ($f = 60$ mm). A beam splitter and an energy meter (Rj 7610, Polytec, Waldbronn, Germany) were used for normalization of the photoacoustic signal. The collimated beam was focused by means of a plano-convex lens ($f = 30$ mm) through the glass window of the flow cell. By the attenuator, the laser pulse energy at the photoacoustic cell could be varied from 100 μ J to 900 μ J.

This setup was used for a detailed investigation of the relationship between photoacoustic signal amplitude and absorption coefficient under reproducible laboratory conditions.

Dye laser system

A tunable, cost efficient, and compact laser system for a practical application of the photoacoustic technique would be a nitrogen-dye laser combination. Since such a laser system was not available during this study, it was simulated by means of a compact dye laser module (LD2C, Laser Photonics, Orlando, USA) which was pumped by a XeCl excimer laser (EMG 201 MSC, Lambda Physik, Göttingen, USA).

The divergent laser beam was collimated by a plano-convex lens ($f = 200$ mm). A beam splitter and an energy meter (Rj 7610, Polytec, Waldbronn, Germany) were used for normalization of the photoacoustic signal. The collimated beam was focused by a plano-convex lens ($f = 30$ mm) and reached the photoacoustic cell.

The wavelength of the emitted radiation could be varied by alignment of the Littrow resonator of the dye laser module. At the beam splitter, 5% of the laser beam intensity was guided to the entrance slit of a double monochromator (H.10 DVIS, Jobin Yvon, Longjumeau Cedex, France) which was coupled with a photomultiplier tube (C956-04, Hamamatsu Photonics, Hamamatsu City, Japan). The output signal of the photomultiplier was recorded by a digital storage oscilloscope (TDS 620, Tektronix, Beaverton, USA).

In this way, the wavelength of the radiation emitted by the dye laser could be determined.

With the laser dye Coumarin 153, the wavelength could be tuned between 520 and 570 nm, and DCM allowed an emission range of 620–680 nm. The laser pulse energy varied between 100 and 300 μ J, depending on the wavelength.

Data analysis

The time-resolved photoacoustic signal consisted of two parts. In relatively low absorbing samples ($\alpha < 6$ cm $^{-1}$), a photoacoustic signal was detected contemporaneously with the laser pulse ($t = 0$) which could be explained by a laser-induced pressure wave generated inside the hydrophone by the transmitted part of the excitation beam. At $t = 400$ ns, an acoustic reflection of the first signal inside the glass window of the hydrophone was observed.

Within a second part of the photoacoustic signal profile beginning at $t = 7$ μ s, pressure waves generated inside the liquid samples were detected. With the acoustic velocity of water (i.e., $c = 1,500$ m s $^{-1}$), the time delay between laser pulse and arrival of the pressure wave at the detector corresponds to a distance of approximately 10 mm which is the distance between entrance window and hydrophone. Therefore it can be concluded, that this part of the signal is generated at the interface between entrance window and liquid sample. As well as in the first part of the photoacoustic signal profile, acoustic reflections at time delays of 400 ns were observed.

For determination of optical absorption coefficients and dye concentrations, the amplitude of the signal at $t = 7$ μ s was evaluated. This value is termed from now on simply “photoacoustic signal amplitude”. The pressure wave generated directly inside the hydrophone by transmitted radiation and its reflections decayed within approximately 2 μ s and did therefore not affect the photoacoustic signal of the sample at $t = 7$ μ s.

Additionally to the optical absorption coefficient, the photoacoustic signal amplitude depends on the laser pulse energy and physical properties of the sample (β , c , and C_p). For samples consisting predominantly of water (e.g., aqueous solutions and biological matrices), the physical properties of water can be assumed. The temperature dependences of C_p , β , and c were corrected by use of literature data [7]. All photoacoustic signal amplitudes were normalized to a laser pulse energy of 1 mJ and a temperature of 25 °C.

Textile dyes

In the experiments presented in this communication, the textile dyes Remazole red RB and Remazole red BS (Hoechst, Frankfurt/M., Germany) were used.

Results and discussion

Calibration of the photoacoustic flow cell

The photoacoustic flow cell was calibrated with solutions of Remazole red RB with concentrations ranging from 150 mg L $^{-1}$ to 30 g L $^{-1}$. For excitation at $\lambda = 532$ nm, a frequency doubled Nd:YAG laser was used. The dye solutions were pumped into the flow cell by a peristaltic pump and the photoacoustic signal amplitude was determined. During the measurement, the pump was turned off. Figure 3 exhibits the plot of the signal amplitudes versus the corresponding dye concentrations. Every dot represents the mean value of 20 repeated photoacoustic measurements.

Contrary to the linear function in Eq. (2), the calibration curve has a sigmoidal shape. As shown in Fig. 4a, the

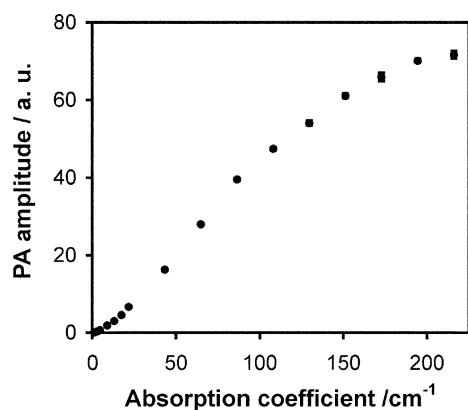


Fig. 3 Calibration curve of the photoacoustic flow cell

plot is approximately parabolic for absorption coefficients lower than 22 cm^{-1} . The IUPAC $3s_B$ criterion resulted in a detection limit of 0.32 cm^{-1} . In the range $22\text{--}108\text{ cm}^{-1}$, the calibration curve is linear (Fig. 4b).

For absorption coefficients larger than 22 cm^{-1} , the optical penetration depth, i.e. the reciprocal value of the absorption coefficient, is in the range of a few $100\text{ }\mu\text{m}$. Therefore, such dye solutions can be characterized as opaque. The irradiated volume is approximately punctiform and therefore a spherical pressure wave is generated. As exhibited in Eq. (2), the amplitude of the spherical wave depends linearly on the concentration. In the range of $108\text{ to }216\text{ cm}^{-1}$, saturation effects lead to deviations from this linear relation. This corresponds to the exponential function in Eq. (1) which can be approximated by a linear function only in the range of $\alpha l < 0.1$. In optical transmission measurements, l is the length of the measurement cell. In the photoacoustic cell described here, the detected signal reflects only a small part of the sample. As described in the Materials and Methods section, the pressure wave is generated at the interface between entrance window and dye solution and is recorded in a time-resolved fashion. Former investigations revealed that the time resolution of photoacoustic detectors based on a $25\text{-}\mu\text{m}$ -thick PVDF film is approximately 7 ns . With the sound velocity of water (i.e., $c = 1,500\text{ m s}^{-1}$), this corre-

sponds to a depth-resolution of $10\text{ }\mu\text{m}$ [8, 9]. With $l = 10\text{ }\mu\text{m}$, α has to be smaller than 100 cm^{-1} in order that the linear approximation in Eq. (2) is valid. This value is in good agreement with our observations. The calibration function deviated from the linear function at $\alpha > 108\text{ cm}^{-1}$.

For absorption coefficients lower than 22 cm^{-1} , the optical penetration depth is in the range of 0.5 up to a few millimeters. The irradiated volume is not punctiform. Therefore, not the whole absorbed energy is converted into a spherical acoustic wave but superpositions of diverse waveforms are generated. Due to this fact, the amplitude of the pressure wave cannot be described by the simple linear relation in Eq. (2). Nevertheless, Fig. 3 reveals that the photoacoustic cell allows the determination of absorption coefficients from the detection limit of 0.32 cm^{-1} up to approximately 220 cm^{-1} —corresponding to Remazol red RB concentrations of 44 mg L^{-1} to 30 g L^{-1} —without any dilution or other kinds of sample preparation.

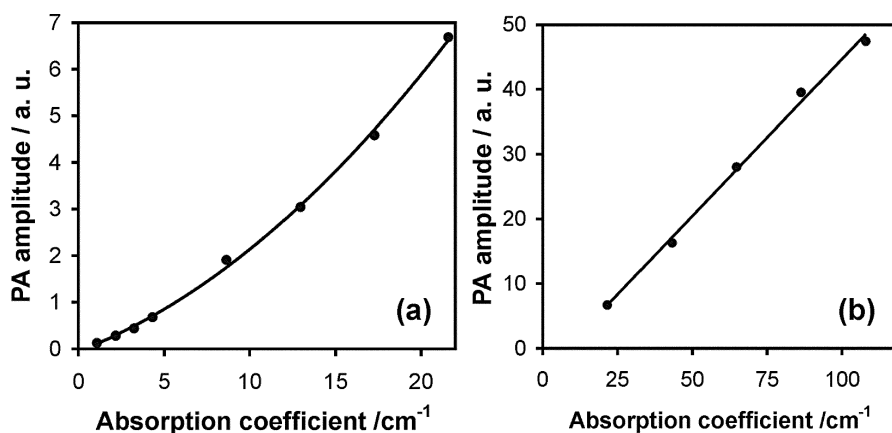
Influence of the flow velocity

After calibration of the photoacoustic cell using a Nd:YAG laser the setup was transferred to a dye laser which was pumped by a XeCl excimer laser. By use of the laser dye Coumarin 153, photoacoustic measurements at $\lambda = 550\text{ nm}$ were performed.

Solutions of the red textile dye Remazole red BS with concentrations ranging from 25 mg L^{-1} to 25 g L^{-1} were pumped through the flow cell and the corresponding photoacoustic signals were recorded. In order to investigate the influence of the flow velocity, all measurements were performed at four different volume flows through the cell, that is, $0, 21, 35,$ and 49 mL min^{-1} .

Figure 5 shows the four calibration curves corresponding to four different volume flows. Every dot represents the mean value of 20 repeated photoacoustic measurements. The curves display the sigmoidal shape of the calibration in Fig. 3 and are in good agreement with each other. Deviations of two signal amplitudes which were measured at 49 mL min^{-1} from the other flow velocities are due to air bubbles present in the flow cell during the

Fig. 4a,b Parabolic calibration function for absorption coefficients smaller than 22 cm^{-1} (a) and linear range of the calibration between 22 and 108 cm^{-1} (b)



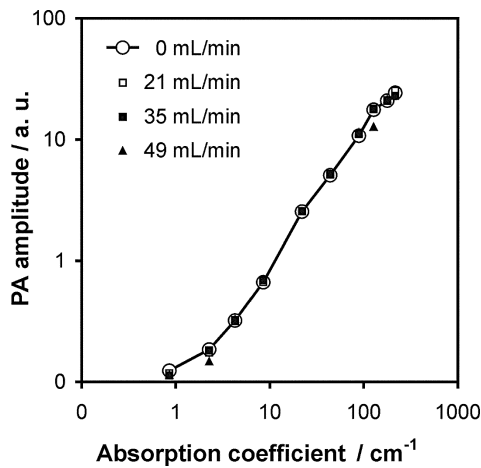


Fig. 5 Influence of the flow velocity on the calibration functions of the photoacoustic flow cell

measurement. It can be concluded that the dye concentration can be determined by photoacoustic measurements independently from the flow velocity.

Additionally, noise generated by the flowing solution did not affect the photoacoustic signal. Noise associated with flowing samples can be a problem when photoacoustic signals are detected by microphones. Within this study, a piezoelectric transducer was used which detects ultrasonic waves with frequencies ranging up to a few 10 MHz. Obviously, the noise of the liquid flow is relatively weak in the ultrasonic range.

Characterization of the flow cell

The response time of the photoacoustic sensor system after a change of the dye concentration was determined by

switching between 5 g L^{-1} Remazole red RB and pure water at the sample inlet of the flow cell. At a volume flow of 30 mL min^{-1} , the calculated mean residence time inside the cell is 1 s. In addition to the residence time, the response time is influenced by the volume of the tubing and by backmixing effects inside tubing and flow cell.

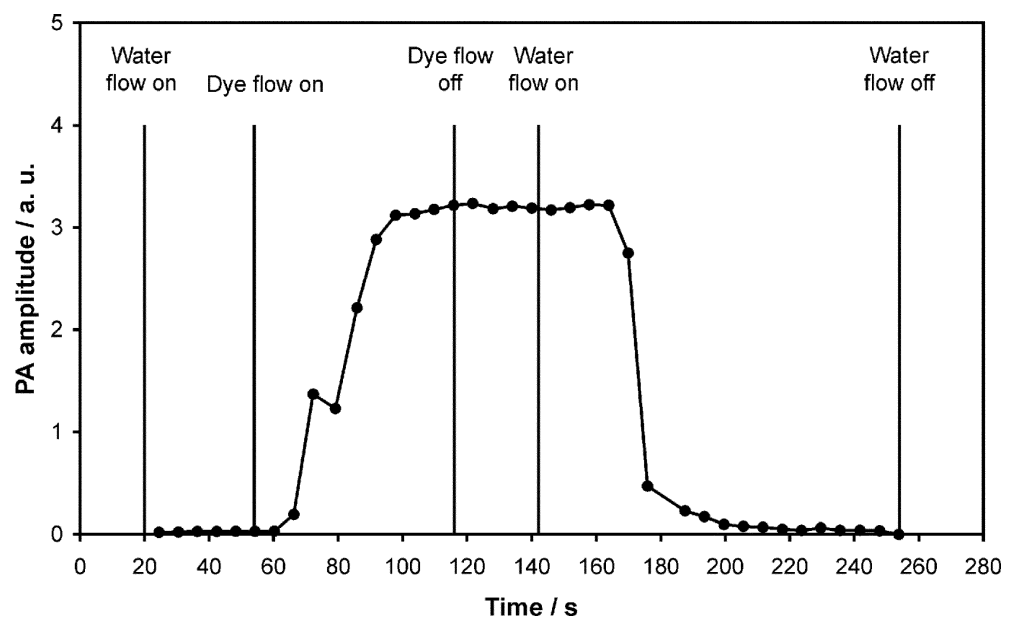
Figure 6 shows the behavior of the photoacoustic signal amplitudes during the experiment. At the beginning ($t=0$) the system was flushed with pure water. During the experiment, photoacoustic measurements were performed at intervals of 6 s. At $t=54 \text{ s}$ the sample inlet was switched from water to the dye solution. At $t=66 \text{ s}$, the signal began to increase and reached a plateau at $t=98 \text{ s}$. At $t=116 \text{ s}$, the pump was turned off. The signal was constant over 26 s. Afterwards, pure water was pumped again through the system. At $t=170 \text{ s}$, the signal began to decrease and reached the noise level at $t=200 \text{ s}$.

For characterization of the temporal behavior of the measurement system, the response time ϑ_{10}^{90} was calculated. ϑ_{10}^{90} is the time delay between the photoacoustic signal with 10% of the maximal amplitude and the signal with 90% of this value. At a volume flow of 30 mL min^{-1} , ϑ_{10}^{90} was $19 \pm 1 \text{ s}$ which corresponds to a volume mixing constant of $9.5 \pm 0.5 \text{ mL}$.

Simulated stirring tank reactor

In order to simulate a process in a textile dyeing plant, a small stirring tank reactor was set up and the mixing of pure water with the red textile dye Remazole red BS and its dilution with water were monitored by on-line measurements with the photoacoustic flow cell. The reactor consisted of a beaker on a magnetic stirrer which contained a constant volume of 100 mL during the whole experiment. By means of a peristaltic pump, textile dye or pure water, respectively, were pumped into the beaker.

Fig. 6 Time characteristics of the photoacoustic flow cell



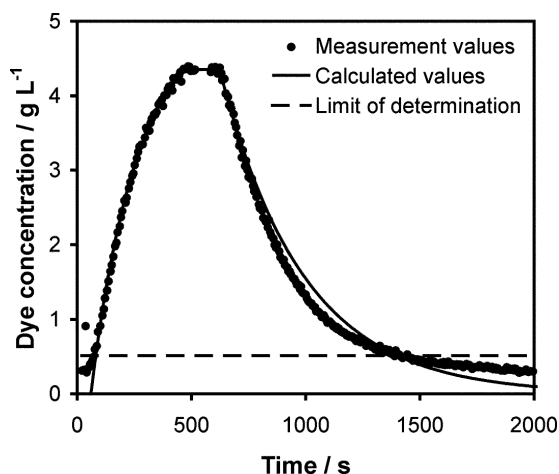


Fig. 7 Dye concentration measured by photoacoustic spectroscopy during the experiments with the simulated stirring tank reactor in comparison with the theoretically calculated trend

Through another channel of the same peristaltic pump, liquid was pumped out of the reactor and through the photoacoustic flow cell. The volume flows at inlet and outlet of the reactor were identical. For excitation at $\lambda = 550$ nm, the dye laser system was used.

At the beginning of the experiment, the system was filled with pure water. The volume flow through the system was 30 mL min^{-1} . Figure 7 exhibits the behavior of the dye concentrations determined by photoacoustic measurements during the experiment.

At $t = 0$ s, a solution of 5 g L^{-1} was pumped into the stirring tank reactor. The signal amplitude increased and reached the limit of determination after 80 s. This time delay reflects the length of the tubing from the dye reservoir to the photoacoustic cell. After 480 s, the pump was turned off. The signal remained constant over 120 s. After 600 s from the start of the experiment, the content of the stirring tank reactor was diluted by pure water with a volume flow of $16.75 \text{ mL min}^{-1}$. The photoacoustic signal amplitude decreased and reached the limit of determination at $t = 1,400$ s.

The trend of the dye concentration was calculated theoretically as explained below and compared with the measurement values. The mean residence time τ inside the reactor can be calculated as the ratio of the reactor volume to the volume flow. The reactor volume was 100 mL. During the addition of textile dye, the volume flow was 30 mL min^{-1} . Therefore, the mean residence time was 3.33 min. The dye concentration inside the system at the moment t can be calculated as

$$c(t) = c_{\max} \left(1 - e^{-\frac{(t-t_0)}{\tau}} \right) \quad (5)$$

where c_{\max} is the maximal concentration which is reached at $t \rightarrow \infty$ and t_0 is the time delay between beginning of the

experiment and increase of the concentration at the measurement cell.

During the dilution of the dye by pure water, the volume flow was $16.75 \text{ mL min}^{-1}$. Thus, the mean residence time was 5.97 min. The concentrations $c(t)$ during the dilution process can be calculated as

$$c(t) = c_{\max} e^{-\frac{(t-t_0)}{\tau}} \quad (6)$$

with t_0 denoting the time delay between start of the experiment and decrease of the dye concentration. In Fig. 7, the theoretical calculated trend is compared with the measurement values. As can be seen, the concentrations determined by photoacoustic measurements are in good agreement with the theory.

Conclusions

This study revealed that photoacoustic spectroscopy allows the monitoring of dye concentration over a wide concentration range without any dilution or other sample preparations. By use of a flow cell, the photoacoustic measurements could be performed in a continuous fashion. In continuous measurements, the signal was not affected by the flow velocity. Changes of the dye concentration could be monitored on-line with a time-resolution of a few seconds. In a small stirring tank reactor, the dye concentration could be monitored during addition of a textile dye and during its dilution by addition of water. The plot of concentration versus time was in good agreement with the theoretically calculated trend.

Acknowledgements The authors acknowledge the financial support by Deutsche Forschungsgemeinschaft and a grant awarded to Thomas Schmid by Max-Buchner-Forschungsstiftung.

References

- Lippert G, Schulze-Braucks M (1989) *Textilveredlung* 24:355–361
- Tam AC (1986) *Rev Mod Phys* 58:381–431
- Tersic M, Jovanovic-Kurepa J, Slivka J (1998) *J Phys D Appl Phys* 31:1366–1374
- Patel CKN, Tam AC (1981) *Rev Mod Phys* 53:517–550
- Emmony DC, Siegrist M, Kneubuehl FK (1976) *Appl Phys Lett* 9:547–549.
- Trusler JPM (1991) *Physical acoustics and metrology of fluids*. Adam Hilger, New York
- Weast RC (1983) *CRC handbook of chemistry and physics*. CRC Press, Boca Raton
- Kopp C, Niessner R (1999) *Anal Chem* 71:4663–4668
- Schmid T, Panne U, Haisch C, Hausner M, Niessner R (2002) *Environ Sci Technol* 36:4135–4141